


**RESEARCH ARTICLE**

# Boroxine benzaldehyde complex for pharmaceutical applications probed by electron interactions

Joao Pereira-da-Silva<sup>1</sup> | Ana Nunes<sup>1</sup> | Monica Mendes<sup>1</sup> | Rodrigo Rodrigues<sup>1</sup> | Lucas Cornetta<sup>2</sup> | Filipe Ferreira da Silva<sup>1</sup> 

<sup>1</sup>CEFITEC, Departamento de Física, NOVA School of Science and Technology, Universidade NOVA de Lisboa, Caparica, Portugal

<sup>2</sup>Instituto de Física Gleb Wataghin, Universidade Estadual de Campinas, Campinas, São Paulo, Brazil

**Correspondence**

F. Ferreira da Silva, CEFITEC, Departamento de Física, NOVA School of Science and Technology, Universidade NOVA de Lisboa, 2829-516 Caparica, Portugal.  
Email: [f.ferreiradasilva@fct.unl.pt](mailto:f.ferreiradasilva@fct.unl.pt)

L. Cornetta, Instituto de Física Gleb Wataghin, Universidade Estadual de Campinas, Campinas, São Paulo, Brazil.  
Email: [lucascor@unicamp.br](mailto:lucascor@unicamp.br)

**Funding information**

Fundação de Amparo à Pesquisa do Estado de São Paulo, Grant/Award Number: 2020/04822-9; Fundação para a Ciência e a Tecnologia, Grant/Award Numbers: PD/00193/2012, PD/BD/14276872018, PTDC/FIS/AQM/31215/2017, UID/FIS/00068/2020

**Rationale:** 2,4,6-Tris(4-formylphenyl)boroxine (TFPB) is a substituted boroxine containing a benzaldehyde molecule bonded to each boron atom. Boroxine cages are an emerging class of functional nanostructures used in host-guest chemistry, and benzaldehyde is a potential radiosensitizer. Reactions initiated by low-energy electrons with such complexes may dictate and bring new fundamental knowledge for biomedical and pharmaceutical applications.

**Methods:** The electron ionization properties of TFPB are investigated using a gas-phase electron-molecule crossed beam apparatus coupled with a reflectron time-of-flight mass spectrometer in an orthogonal geometry. Ionization and threshold energies are experimentally determined by mass spectra acquisition as a function of the electron energy.

**Results:** The abundance of the molecular precursor cation in the mass spectrum at 70 eV is significantly lower than that of the most abundant fragment  $C_7H_5O^+$ . Twenty-nine cationic fragments with relative intensities >2% are detected and identified. The appearance energies of six fragment cations are reported, and the experimental first ionization potential is found at  $9.46 \pm 0.11$  eV. Moreover, eight double cations are identified. The present results are supported by quantum chemical calculations based on bound state techniques, electron ionization models and thermodynamic thresholds.

**Conclusions:** According to these results, the TFPB properties may combine the potential radiosensitizer effect of benzaldehyde with the stability of the boroxine ring.

## 1 | INTRODUCTION

Alongside the relevance in plasma physics, atmospheric sciences, astrophysics and many other fields, the study of electron-molecule interactions at low energies is also motivated by the sparse track of secondary electrons created by the interaction of high-energy radiation in a biological medium,<sup>1,2</sup> which is an

interesting feature for radiotherapy. The sensitivity of tumors to high-energy radiation together with the generated secondary species is enhanced by the use of chemoagents known as radiosensitizers. In summary, the effect of secondary electrons in the cell environment is ultimately linked to the radiation damage to DNA and other biomolecules, which is supported by several studies.<sup>3-5</sup>

This is an open access article under the terms of the [Creative Commons Attribution-NonCommercial-NoDerivs](https://creativecommons.org/licenses/by-nc-nd/4.0/) License, which permits use and distribution in any medium, provided the original work is properly cited, the use is non-commercial and no modifications or adaptations are made.

© 2022 The Authors. *Rapid Communications in Mass Spectrometry* published by John Wiley & Sons Ltd.

Among the outcomes of the interaction between low-energy electrons (LEEs) and biomolecules, two mechanisms can be highlighted depending on the energy range. At very low collision energies (units of eV), electrons can be attached to neutral targets and form reactive temporary negative ions, or resonances, whose dynamics can be usually viewed as a competition between auto-detachment and nuclear relaxation on the femtosecond scale.<sup>6,7</sup> In the context of radiosensitizers, the temporary negative ions can be dissociative and may decay via dissociative electron attachment (DEA).<sup>6–8</sup> However, if the energy of the incident electron is above the ionization threshold of the target, electron-impact ionization becomes prevalent, in comparison to electron attachment, and gradually dominates the total cross-section for electron–molecule scattering. According to Sanche and coworkers,<sup>1</sup> when plasmid DNA is irradiated with electrons above 30 eV, cationic fragments can be formed after the precursor ionization and subsequently damage DNA segments.

Some recent studies have shown the efficiency of LEEs in inducing dissociation in electrophilic compounds through DEA mechanisms yielding reactive radicals that cause DNA damage.<sup>4,5</sup> In recent gas-phase studies, benzaldehyde has been investigated as a potential radiosensitizer by analyzing single electron–molecule interactions.<sup>9</sup> These studies, supported by quantum chemical calculations, suggested rich fragmentation patterns leading to the formation of a vast number of anions.<sup>9</sup> Besides, boroxines, also known as boronic acid anhydrides, are the dehydration products of organoboronic acids.<sup>10</sup> Recent studies have been conducted to understand the structural interconversion mechanisms of boroxine cages containing pyridine that will enable the optimization of several properties such as porosity and size-selective molecular recognition.<sup>11,12</sup> Besides, in previous gas-phase studies, different substituted boroxines were irradiated with electrons above the ionization potential,<sup>13,14</sup> and one DEA study was also performed on triphenylboroxine.<sup>15</sup> In these studies, triphenylboroxine was demonstrated to be stable towards fragmentation upon electron interaction,<sup>15</sup> and the stability of boroxines is affected by the substituent on the boron atom.<sup>13</sup>

2,4,6-Tris(4-formylphenyl)boroxine (TFPB) is a substituted boroxine containing a benzaldehyde molecule bonded to each boron atom. Benzaldehyde is an aromatic aldehyde used in the food, cosmetic and chemical industries.<sup>16</sup> In addition, due to its chemotherapeutic potential and low toxicity, it has been investigated in patients with advanced carcinomas.<sup>17,18</sup> Several *in vitro*<sup>18,19</sup> and *in vivo*<sup>20</sup> studies have been conducted to assess the anticancer effect of benzaldehyde and its derivatives as well as to understand the mechanism of action at the cellular level. Two antitumor mechanisms of benzaldehyde were proposed, namely inhibition of essential nutrient uptake in cancer cells<sup>21</sup> and inhibition of glutathione peroxidase.<sup>22,23</sup> The latter mechanism induces an increase of oxidative stress related to the production of highly reactive oxygen species.

Considering the stability of triphenylboroxine and the potential radiosensitizer effect of benzaldehyde, a deeper knowledge of LEE interactions with TFPB may help to develop new chemo-radiotherapy approaches and protocols. In the present paper, we report the

positive ion formation upon electron interactions in the gas phase with TFPB using a crossed electron–molecule beam setup composed of a trochoidal electron monochromator (TEM) coupled with an orthogonal reflectron time-of-flight mass spectrometer (OReTOFMS). Ionization efficiency curves for the most abundant fragment cations were obtained for energies between 4 and 40 eV with experimental determination of threshold energies. Additionally, at 70 eV, was recorded a mass spectrum.

## 2 | EXPERIMENTAL SETUP

The present study was performed using an experimental setup composed of a trochoidal electron monochromator coupled with an OReTOFMS, described in detail elsewhere.<sup>24</sup> The electrons are emitted from a tungsten hairpin filament, and a quasi-monoenergetic electron beam is generated due to an electric field orthogonal to the magnetic field. The stability of this quasi-monoenergetic electron beam with a resolution of about 180 meV was constantly monitored by a picoampere meter connected to a Faraday plate (*ca* 100 nA for electron energy of 70 eV). Upon the interaction electrons and molecules, ions are formed and then extracted using an extraction field (*ca* 1 V/cm) into the ion guide and further mass-separated in the OReTOFMS (*ca* 800  $m/\Delta m$ ) and detected by a microchannel plate detector.

## 3 | MATERIALS AND METHODS

4-Formylphenylboronic acid (FPBA) was purchased from Sigma-Aldrich with stated purity of 95%. The conversion of FPBA to TFPB is a dehydration reaction driven thermally (Figure 1).

When a sample is heated, FPBA undergoes a dehydration process forming the trimeric anhydride. At the typical experimental base pressure of about  $5 \times 10^{-5}$  Pa, the sample oven was heated to 40°C in order to achieve sufficient sublimation of TFPB. An effusive beam of molecules was formed by a capillary (1 mm in diameter) assembled onto the oven. The ionization energy and threshold energies were experimentally determined using a fitting method based on the Wannier law, and the energy scale was calibrated using the ionization efficiency curve of  $\text{Ar}^+$ , determined by Weitzel et al.<sup>25</sup>

## 4 | DISCUSSION

### 4.1 | Positive ion formation

Figure 2 shows the positive mass spectrum of TFPB recorded at an incident electron energy of 70 eV.

At 70 eV the processes are well above the ionization threshold of the TFPB molecule; therefore, several fragmentation pathways are accessible at this energy. All fragment peaks were assigned according to the isotopic distribution of the elements, including the natural

**FIGURE 1** Dehydration reaction of 4-formylphenylboronic acid to 2,4,6-tris(4-formylphenyl)boroxine

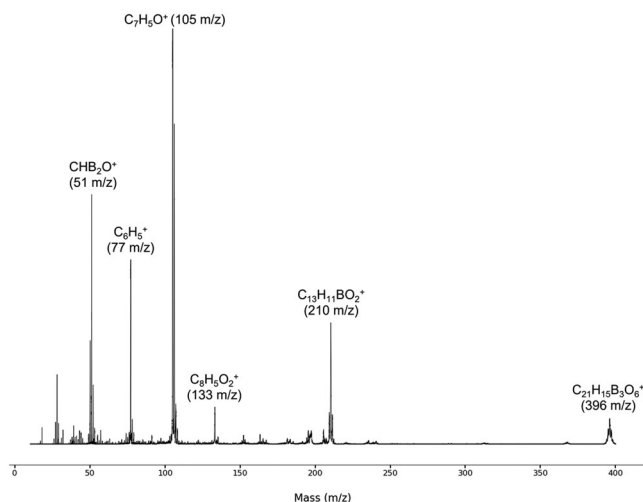
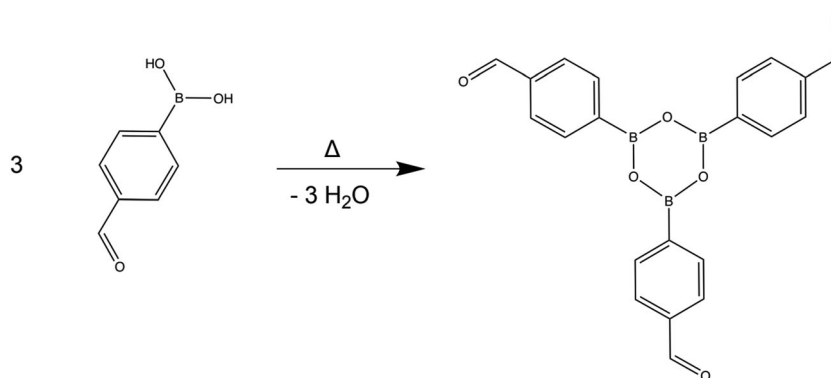


**FIGURE 2** TFPB ( $C_{21}H_{15}B_3O_6$ ) electron ionization mass spectrum recorded at 70 eV incident electron energy.

abundance of  $^{10}B/^{11}B$ . In addition, all cationic peak intensities were normalized according to the  $C_7H_5O^+$  peak signal, which is the most abundant fragment. As far as the authors are aware, no mass spectra obtained by electron ionization have been reported previously.

Comparing the 70 eV spectra of TFPB and triphenylboroxine,<sup>15</sup> the precursor cation's relative intensity is significantly lower for TFPB. In the case of triphenylboroxine the most intense cation is the precursor cation followed by  $Ph_2(C_6H_4)B_2O_2^+$  ( $m/z$  207) with relative intensity of 0.16. In the present case of TFPB, the most intense fragment is  $C_7H_5O^+$  ( $m/z$  105), and precursor cation is formed with a relative intensity of 0.06. In the triphenylboroxine electron ionization mass spectrum, the precursor cation is the most intense fragment. On the other hand, in the TFPB spectrum the precursor cation presents a relative peak intensity of 6%. This indicates that the presence of the formyl group attached to the benzene ring (benzaldehyde) induces molecular instability and, thus, a wide range of fragmentation patterns. The list of 29 cationic fragments with relative intensities >2% is presented in Table 1.

It is also important to remark that the two most abundant cations,  $C_7H_5O^+$  ( $m/z$  105) and  $C_7H_6O^+$  ( $m/z$  106), do not include boron in their chemical structure. This suggests that the boroxine ring is significantly preserved upon electron ionization. We do not discard

**TABLE 1** List of cationic fragments with relative intensities >2% under electron ionization at 70 eV electron energy

Cation	$m/z$	Relative intensity
$(PhCBO_3)_3^+$	396	0.06
$C_{20}H_{14}B_3O_5^+$	367	0.01
$C_{13}H_{12}BO_2^+$	211	0.07
$C_{13}H_{11}BO_2^+$	210	0.29
$C_{12}H_{13}O_3^+$	205	0.04
$C_9H_8B_3O_3^+$	197	0.03
$C_{11}H_9B_2O_2^+$	195	0.03
$C_7H_4B^+$	163	0.02
$C_7H_9BO_3^+$	152	0.02
$C_8H_5O_2^+$	133	0.09
$C_7H_7O^+$	107	0.01
$C_7H_6O^+$	106	0.75
$C_7H_5O^+$	105	1
$C_4BO_2^+$ or $C_5H_4BO^+$	91	0.02
$C_6H_5^+$	77	0.43
$C_3H_2B_2O^+$	76	0.03
$C_5H_3B^+$ or $CH_3BO_3^+$	74	0.03
$CH_2BO_2^+$	57	0.03
$CBO_2^+$	55	0.02
$C_2H_2BO^+$	53	0.04
$C_2B_2H_5^+$ or $C_2HBO^+$	52	0.14
$CHB_2O^+$	51	0.59
$HBO_2^+$ or $C_2H_4O^+$	44	0.03
$BO_2^+$	43	0.03
$HB_2O^+$	39	0.04
$O_2^+$	32	0.03
$CHO^+$	29	0.05
$N_2^+$	28	0.15
$BO^+$	27	0.05

the possibility of electronic rearrangements, although  $C_7H_5O^+$  can be formed by simple cleavage of C&B bond and  $C_7H_6O^+$  by the cleavage of C-B bond followed by proton transfer. In addition, eight double cationic fragments are formed (Table 2). The double cations have been assigned regarding  $^{10}B$  isotopic contribution. Precursor

double cation is attributed at  $m/z$  197.5; double cation  $C_{13}H_{12}BO_2^{2+}$  ( $m/z$  105.5) corresponds to the double ionization of cationic species  $m/z$  211.

Double cation  $m/z$  82.5 is assigned as  $C_6H_7B_2O_4^{2+}$ ;  $m/z$  77.5,  $m/z$  53.5 and  $m/z$  52.5 are assigned to the double cationic species  $C_8H_5B_2O_2^{2+}$ ,  $C_7H_6O^{2+}$  and  $C_7H_5O^{2+}$ , respectively. The latter two correspond to the double ionization of  $C_7H_6O^+$  and  $C_7H_5O^+$ ,  $m/z$  107 and  $m/z$  106 respectively. The only boron-absent double cation identified appears at  $m/z$  38.5 being attributed to the phenyl double cation  $C_6H_5^{2+}$ . The lightest identified double cation is attributed to  $C_5H_3O^{2+}$  ( $m/z$  37.5).

**TABLE 2** List of the observed double-ionized cationic fragments

Cation	$m/z$
$C_{21}H_{15}B_3O_6^{2+}$	197.5
$C_{13}H_{12}BO_2^{2+}$	105.5
$C_6H_7B_2O_4^{2+}$	82.5
$C_8H_5B_2O_2^{2+}$	77.5
$C_7H_6O^{2+}$	53.5
$C_7H_5O^{2+}$	52.5
$C_6H_5^{2+}$	38.5
$C_5H_3B^{2+}$	37.5

## 4.2 | Minor fragments

Apart from the four cations described in Table 1, there were identified 18 more fragments with relative intensities  $<2\%$ . The fragment cations  $C_{18}H_{15}B_3O_3^+$  ( $m/z$  312),  $C_{13}H_{14}B_2O_3^+$  ( $m/z$  240),  $C_{14}H_{13}B_2O_2^+$  ( $m/z$  235),  $C_{15}H_2B_2O^+$  ( $m/z$  220),  $C_{12}H_9B_2O_2^+$  ( $m/z$  207),  $C_{12}H_9O_2^+$  ( $m/z$  185),  $C_9H_5B_2O_3^+$  ( $m/z$  183),  $C_{11}H_6BO_2^+$  ( $m/z$  181),  $C_6H_9B_2O_4^+$  ( $m/z$  167),  $C_6H_7B_2O_4^+$  ( $m/z$  165),  $C_{10}H_6BO^+$  ( $m/z$  152),  $C_6H_4BO_3^+$  ( $m/z$  135),  $C_2HB_2O_4^+$  ( $m/z$  111),  $CBO_3^+$  ( $m/z$  71),  $CHO_2^+$  ( $m/z$  45),  $C_2HO^+$  ( $m/z$  41) and  $CH_3O^+$  or  $H_4BO^+$  ( $m/z$  31) are reported in this electron ionization study.

## 4.3 | Ionization and appearance energies

The ionization efficiency curves near the threshold were measured for six abundant cations in the mass spectrum at 70 eV. The experimental data of cations  $m/z$  51,  $m/z$  77,  $m/z$  91,  $m/z$  105,  $m/z$  210 and  $m/z$  396 were fitted by the method based on the Wannier law<sup>14</sup> to determine the experimental ionization and appearance energies. The experimental ionization energy of TFPB was determined at  $9.46 \pm 0.11$  eV. Figure 3 depicts the experimental data and the respective Wannier-type fits for the six most intense cations.

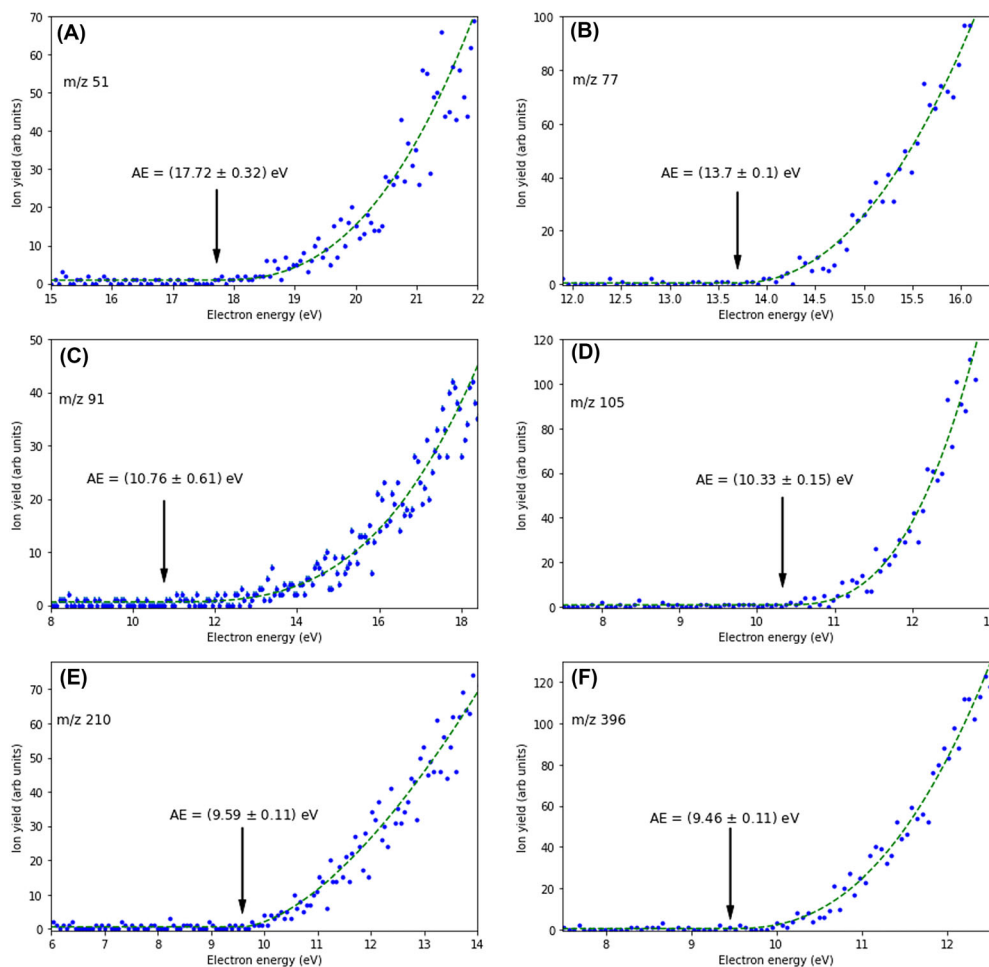
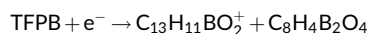


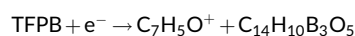
**FIGURE 3** Experimental thresholds for the six most abundant cations. The blue dots represent the experimental data and the green dashed line represents the Wannier-type fitting function. The values in parentheses correspond to the experimental threshold along with the respective statistical uncertainties. (A)  $CHB_2O^+$  ( $m/z$  51); (B)  $C_6H_5^+$  ( $m/z$  77); (C)  $C_4BO^+$  or  $C_5H_4BO^+$  ( $m/z$  91); (D)  $C_7H_5O^+$  ( $m/z$  105); (E) precursor cation  $C_{13}H_{11}BO_2^+$  ( $m/z$  210); (F) precursor cation  $C_{21}H_{15}B_3O_6^+$  ( $m/z$  396) [Color figure can be viewed at [wileyonlinelibrary.com](http://wileyonlinelibrary.com)]

The appearance energy of  $C_7H_5O^+$  ( $m/z$  105), which is assigned to C&B bond cleavage (bond break between the benzaldehyde and the boroxine ring), was found at  $10.33 \pm 0.15$  eV. The appearance energy of phenyl cation ( $m/z$  77) that is related to the cleavage of the formyl group and the C&B bond was observed at  $10.7 \pm 0.1$  eV. The remaining appearance energies of the other cations  $CHB_2O^+$  ( $m/z$  51),  $C_{13}H_{11}BO_2^+$  ( $m/z$  210) and  $C_4BO^+$  or  $C_5H_4BO^+$  ( $m/z$  91) were determined at  $17.72 \pm 0.32$ ,  $9.59 \pm 0.11$  and  $10.76 \pm 0.61$  eV, respectively.

Theoretical values for the first ionization potentials (IPs) were determined using the outer-valence Green's function (OVGF) method, together with the 6-311G(df,p) basis set. The calculations were performed with the *gaussian09* package.<sup>26</sup> In this approach, the IPs correspond to the absolute values of the OVGF energies of the molecular orbitals of the neutral molecule. The first IP was obtained at 9.49 eV, which is in very good agreement with the appearance energy of the precursor cation ( $m/z$  396). Besides, we conducted auxiliary investigation of the dissociation thresholds associated with some of the most abundant singly ionized fragments, from which we drew a conclusion that is worth mentioning. Due to the complexity of the molecule, we only focused on reactions involving single bond breaks and/or the simplest possible rearrangements. The thresholds were calculated with the G4(MP2) methodology, as implemented in *gaussian09*, at  $T = 313$  K. For the cationic fragment  $m/z$  210, our estimate for the reaction



is  $\Delta E_{th} = 10.77$  eV, which is more than 1 eV higher than the observed appearance energy for that channel. A similar discrepancy was observed for the cationic fragment  $m/z$  105. The calculated threshold for the reaction



corresponding to a single C&B bond break was  $\Delta E_{th} = 11.89$  eV, about 1.56 eV above the value observed experimentally. These results indicate that parallel reactions may take place. Along the dissociation paths, secondary rearrangements with more than two products should occur, therefore lowering the reaction threshold. As suggested, a parallel reaction leading to formation of boroxine  $H_3B_3O_3$  is exothermic by 1217.54 kJ/mol.<sup>27</sup> The energy release in a possible lateral reaction will contribute to the thermodynamics lowering. This fact may explain the difference between experimental and theoretical values.

## 5 | CONCLUSIONS

TFPB shows rich fragmentation patterns upon electron interactions at 70 eV, including several double-ionization cations. The precursor cation's relative intensity is significantly lower compared to the most abundant fragment  $C_7H_5O^+$ , which indicates that the presence of

benzaldehyde as a substituent on the boron atom induces molecular instability when compared to triphenylboroxine (phenyl groups as substituents). Twenty-nine cationic fragments with relative intensities  $> 2\%$  were detected and identified. The ionization energy of TFPB was found at  $9.46 \pm 0.11$  eV. In addition, it was observed that three of the most intense cationic fragments do not include boron in their molecular composition, suggesting the boroxine ring's stability. Thus, these results suggest that the TFPB properties may combine the potential radiosensitizer effect of benzaldehyde with the stability of the boroxine ring, which might be important in drug delivery. This comprehensive description of electron-induced dissociation of TFPB may contribute to the development of novel medical strategies, namely in anticancer therapy, including chemo-radiotherapy protocols.

## ACKNOWLEDGMENTS

The authors acknowledge Professor Pedro M. P. Gois for support and constructive discussions, from the iMed.Ulisboa - Institute for Medicines and Pharmaceutical Sciences, Faculty of Pharmacy, Universidade de Lisboa. J.P.S. acknowledges FCT-MCTES through PhD grant PD/BD/142768/2018, and M.M., A.N., R.R. and F.F.S. acknowledge the Portuguese National Funding Agency FCT-MCTES through research grant PTDC/FIS-AQM/31215/2017. L.C. acknowledges financial support from São Paulo Research Foundation (FAPESP), under grant N.2020/04822-9. This work was also supported by Radiation Biology and Biophysics Doctoral Training Programme (RaBBiT, PD/00193/2012); UID/Multi/04378/2019 (UCIBIO); UID/FIS/00068/2020 (CEFITEC).

## PEER REVIEW

The peer review history for this article is available at <https://publons.com/publon/10.1002/rcm.9418>.

## DATA AVAILABILITY STATEMENT

The data that support the findings of this study are available from the corresponding author upon reasonable request.

## ORCID

Filipe Ferreira da Silva  <https://orcid.org/0000-0002-2182-2965>

## REFERENCES

- Dong Y, Liao H, Gao Y, Cloutier P, Zheng Y, Sanche L. Early events in radiobiology: Isolated and cluster DNA damage induced by initial cations and nonionizing secondary electrons. *J Phys Chem Lett*. 2021; 12(1):717-723. doi:10.1021/acs.jpcclett.0c03341
- Boudaïffa B, Cloutier P, Hunting D, Huels MA, Sanche L. Resonant formation of DNA strand breaks by low-energy (3 to 20 eV) electrons. *Science* (80-). 2000;287(5458):1658-1660. doi:10.1126/science.287.5458.1658
- Meißner R, Feketeová L, Ribar A, Fink K, Limão-Vieira P, Denifl S. Electron ionization of imidazole and its derivative 2-nitroimidazole. *J Am Soc Mass Spectrom*. 2019;30(12):2678-2691. doi:10.1007/s13361-019-02337-w
- Schürmann R, Tsering T, Tanzer K, Denifl S, Kumar SVK, Bald I. Resonante Bildung von Strangbrüchen in sensibilisierten

- Oligonukleotiden induziert durch niederenergetische Elektronen (0.5-9.0 eV). *Angew Chem*. 2017;129(36):11094-11098. doi:10.1002/ange.201705504
5. Rak J, Chomicz L, Wiczek J, et al. Mechanisms of damage to DNA labeled with electrophilic nucleobases induced by ionizing or UV radiation. *J Phys Chem B*. 2015;119(26):8227-8238. doi:10.1021/acs.jpcc.5b03948
  6. Marton L. *Advances in Electronics and Electron Physics*. Vol. 46. Academic Press; 1978.
  7. Christophorou LG. *Fundamental Electron Interactions with Plasma Processing Gases*. Kluwer Academic; 2004. doi:10.1007/978-1-4419-8971-0
  8. Alizadeh E, Orlando TM, Sanche L. Biomolecular damage induced by ionizing radiation: The direct and indirect effects of low-energy electrons on DNA. *Annu Rev Phys Chem*. 2015;66(December):379-398. doi:10.1146/annurev-physchem-040513-103605
  9. Ameixa J, Arthur-Baidoo E, Pereira da Silva J, et al. Formation of resonances and anionic fragments upon electron attachment to benzaldehyde. *Phys Chem Chem Phys*. 2020;22(15):8171-8181. doi:10.1039/d0cp00029a
  10. Tokunaga Y. Boroxine chemistry: From fundamental studies to applications in supramolecular and synthetic organic chemistry. *Heterocycles*. 2013;87(5):991-1021. doi:10.3987/REV-13-767
  11. Beuerle F, Gole B. Covalent organic frameworks and cage compounds: Design and applications of polymeric and discrete organic scaffolds. *Angew Chem Int Ed*. 2018;57(18):4850-4878. doi:10.1002/anie.201710190
  12. Ono K, Shimo S, Takahashi K, Yasuda N, Uekusa H, Iwasawa N. Dynamic interconversion between boroxine cages based on pyridine ligation. *Angew Chem*. 2018;130(12):3167-3171. doi:10.1002/ange.201713221
  13. Cragg RH, Todd JFJ, Weston AF. Mass spectra of organoboron compounds - II: The mass spectra of triphenylboroxine and its precursor phenylboronic acid. *Org Mass Spectrom*. 1972;6(10):1077-1081. doi:10.1002/oms.1210061004
  14. Wannier GH. Physical review the threshold law for single ionization of atoms or ions by electrons. *Phys Rev*. 90:817-825.
  15. Pereira-da-Silva J, Mendes M, Nunes A, Araújo J, Cornetta LM, da Silva F. Triphenylboroxine stability under low energy electron interactions. *Phys Chem Chem Phys*. 2022;24(17):10025-10032. doi:10.1039/D2CP00855F
  16. Demir E, Kocaoğlu S, Kaya B. Assessment of genotoxic effects of benzyl derivatives by the comet assay. *Food Chem Toxicol*. 2010;48(5):1239-1242. doi:10.1016/j.fct.2010.02.016
  17. Takeuchi S, Kochi M, Sakaguchi K, Nakagawa K, Mizutani T. Benzaldehyde as a carcinostatic principle in figs. *Agric Biol Chem*. 1978;42:1449-1451.
  18. Ariyoshi-Kishino K, Hashimoto K, Amano O, Saitoh J, Kochi M, Sakagami H. Tumor-specific cytotoxicity and type of cell death induced by benzaldehyde. *Anticancer Res*. 2010;30(12):5069-5076.
  19. Liu Y, Sakagami H, Hashimoto K, et al. Tumor-specific cytotoxicity and type of cell death induced by beta-cyclodextrin benzaldehyde inclusion compound. *Anticancer Res*. 2008;28(1A):229-236.
  20. Ochiai H, Niwayama S, Masuyama K. Inhibition of experimental pulmonary metastasis in mice by fl-cyclodextrin-benzaldehyde. *J Cancer Res Clin Oncol*. 1986;112(3):216-220. doi:10.1007/BF00395915
  21. Watanuki M, Sakaguchi K. Selective inhibition by benzaldehyde of the uptake of nucleosides and sugar into simian virus 40-transformed cells. *Cancer Res*. 1980;40:2574-2579.
  22. Tabatabaie T, Floyd RA. Inactivation of glutathione peroxidase by benzaldehyde. *Toxicol Appl Pharmacol*. 1996;141(2):389-393. doi:10.1006/taap.1996.0304
  23. Ulker Z, Alpsoy L, Mihmanli A. Assessment of cytotoxic and apoptotic effects of benzaldehyde using different assays. *Hum Exp Toxicol*. 2013;32(8):858-864. doi:10.1177/0960327112470271
  24. Pereira-Da-Silva J, Rodrigues R, Ramos J, et al. Electron driven reactions in tetrafluoroethane: Positive and negative ion formation. *J Am Soc Mass Spectrom*. 2021;32(6):1459-1468. doi:10.1021/jasms.1c00057
  25. Weitzel K-M, Mzhnert J, Penno M. ZEKE-PEPICO investigations of dissociation energies in ionic reactions. *Chem Phys Lett*. 1994;224(3-4):371-380. doi:10.1016/0009-2614(94)00567-2
  26. Frisch MJ, Trucks GW, Schlegel HB, et al. Gaussian 09, Revision D.01. 2009.
  27. Chase MW. NIST-JANAF Thermochemical Tables, 4th edition. *J Phys Chem Ref Data, Monogr*. 1998;9:1-1951.

**How to cite this article:** Pereira-da-Silva J, Nunes A, Mendes M, Rodrigues R, Cornetta L, Ferreira da Silva F. Boroxine benzaldehyde complex for pharmaceutical applications probed by electron interactions. *Rapid Commun Mass Spectrom*. 2023;37(1):e9418. doi:10.1002/rcm.9418